Faraday Discussions
Cite this: DOI: 10.1039/c5fd00231a

PAPER



# Electrolysis of metal oxides in $MgCl_2$ based molten salts with an inert graphite anode

Yating Yuan,[a] Wei Li,[a] Hualin Chen,[a] Zhiyong Wang,[a] Xianbo Jin*[a] and George Z. Chen[b]

Received 20th December 2015, Accepted 22nd January 2016
DOI: 10.1039/c5fd00231a

Electrolysis of solid metal oxides has been demonstrated in $MgCl_2$–NaCl–KCl melt at 700 °C taking the electrolysis of $Ta_2O_5$ as an example. Both the cathodic and anodic processes have been investigated using cyclic voltammetry, and potentiostatic and constant voltage electrolysis, with the cathodic products analysed by XRD and SEM and the anodic products by GC. Fast electrolysis of $Ta_2O_5$ against a graphite anode has been realized at a cell voltage of 2 V, or a total overpotential of about 400 mV. The energy consumption was about 1 kW h $kg_{Ta}^{-1}$ with a nearly 100% Ta recovery. The cathodic product was nanometer Ta powder with sizes of about 50 nm. The main anodic product was $Cl_2$ gas, together with about 1 mol% $O_2$ gas and trace amounts of CO. The graphite anode was found to be an excellent inert anode. These results promise an environmentally-friendly and energy efficient method for metal extraction by electrolysis of metal oxides in $MgCl_2$ based molten salts.



## Introduction

Metal materials are crucial to our society. Metals are mainly produced by pyro-metallurgical methods such as carbothermic or metallothermic reductions. However, these processes usually involve multiple steps, and are energy intensive and environmentally unfriendly.[1,2] At the end of the twentieth century, Chen *et al.*[3] proposed the solid electrochemical reduction of $TiO_2$ to produce Ti in $CaCl_2$ molten salt, known as the FFC Cambridge process. Since then, this process has received much attention. Up till now, many metals, semi-metals and their alloys have been successfully prepared by this simple solid oxide reduction process.[4,5] The FFC Cambridge process can be summarized by following reactions.

Overall reaction:

$$MO_x \rightarrow M + x/2O_2 \text{ (inert anode)} \quad (1a)$$

[a]College of Chemistry and Molecular Sciences, Hubei Key Laboratory of Electrochemical Power Sources, Wuhan University, Wuhan, 430072, P. R. China. E-mail: xbjin@whu.edu.cn; Fax: +86 27 68756319; Tel: +86 27 68756319
[b]Department of Chemical and Environmental Engineering, Faculty of Engineering, The University of Nottingham, Nottingham, NG7 2RD, UK

$$nMO_x + xC \rightarrow nM + xCO_n \text{ (carbon anode, } n = 1 \text{ or } 2) \quad (1b)$$

Cathodic reaction:

$$MO_x + 2xe \rightarrow M + xO^{2-} \quad (2)$$

Anodic reaction:

$$2O^{2-} \rightarrow O_2 + 2e \text{ (inert anode)} \quad (3a)$$

$$nO^{2-} + C \rightarrow CO_n + 2ne \text{ (carbon anode)} \quad (3b)$$

In the above equations M represents the studied metal (*e.g.* Ti, Nb and Ta) or semi-metal (*e.g.* Si).

During electrolysis, the graphite anode is often used for its good electronic and mechanical properties. However, as shown by Reaction (3b), the anodic discharge of dissolved $O^{2-}$ ions in $CaCl_2$, which come from the cathode by Reaction (2), will lead to anode consumption and consequently carbon emission. Moreover, the $CO_2$ produced at the anode can react with $O^{2-}$ ions in the molten salt to form $CO_3^{2-}$ ions, which will move back to the cathode and discharge to carbon and $O^{2-}$ ions,[6,7] leading to carbon contamination to the metal product, floating carbon on the surface of $CaCl_2$ melt, as well as low current efficiency. Although many inert anodes have been developed for $O_2$ evolution,[8–12] they are yet pending for commercial verification. At present, similar to the electrolysis of dissolved $Al_2O_3$ in cryolite based molten fluorides, carbon anodes are still the choice for the electrolysis of solid metal oxides in molten $CaCl_2$. To deal with the relevant problems, recently we have proposed a "disengaging strategy" by electrolysis of solid metal oxides in $MgCl_2$ based molten salts, in which the solubility of $O^{2-}$ ions is insignificant to transport $O^{2-}$ to the anode.[13] Alternatively, the released $O^{2-}$ ions stay in the cathode by forming MgO precipitation, and the anode reaction is thus changed to oxidation of $Cl^-$ ions to the $Cl_2$ gas. This disengaging strategy makes the carbon anode effectively non-consumable, eliminating $CO_2$ emission and all related problems. Our new process can be represented by Reactions (4–6).

Overall reaction:

$$MO_x + xMgCl_2 = M + xMgO + xCl_2 \quad (4)$$

Cathodic reaction:

$$MO_x + xMgCl_2 + 2xe \rightarrow M + xMgO + 2xCl^- \quad (5)$$

Anodic reaction:

$$2xCl^- \rightarrow xCl_2 + 2xe \quad (6)$$

As indicated in Table 1, this new process, thermodynamically, can be applied to reduce most transitional metal oxides to respective metals, including some rare earth metals, such as uranium.

Considering molten $MgCl_2$ by itself has a relatively high vapor pressure, it is better to be used together with other chloride salts, such as NaCl and KCl. Using

 

Table 1 Standard decomposition voltages of metal oxides in molten $MgCl_2$ at 700 °C, calculated from HSC Chemistry 6 (A. Roine, HSC Chemistry 6, Outotec Research Oy, 2006)

| Metal oxides | Decomposition voltage (V) |
|---|---|
| $2KCl = 2K + Cl_2(g)$ | 3.566 |
| $2NaCl = 2Na + Cl_2(g)$ | 3.329 |
| $MgCl_2 = Mg + Cl_2(g)$ | 2.534 |
| $2MgCl_2 + HfO_2 = Hf + 2MgO + 2Cl_2(g)$ | 2.388 |
| $2MgCl_2 + UO_2 = U + 2MgO + 2Cl_2(g)$ | 2.335 |
| $2MgCl_2 + ZrO_2 = Zr + 2MgO + 2Cl_2(g)$ | 2.317 |
| $2MgCl_2 + TiO_2 = Ti + 2MgO + 2Cl_2(g)$ | 1.949 |
| $2MgCl_2 + SiO_2 = Si + 2MgO + 2Cl_2(g)$ | 1.865 |
| $3MgCl_2 + B_2O_3 = 2B + 3MgO + 3Cl_2(g)$ | 1.731 |
| $5MgCl_2 + Ta_2O_5 = 2Ta + 5MgO + 5Cl_2(g)$ | 1.638 |
| $3MgCl_2 + V_2O_3 = 2V + 3MgO + 3Cl_2(g)$ | 1.616 |
| $5MgCl_2 + Nb_2O_5 = 2Nb + 5MgO + 5Cl_2(g)$ | 1.488 |
| $3MgCl_2 + Cr_2O_3 = 2Cr + 3MgO + 3Cl_2(g)$ | 1.478 |
| $3MgCl_2 + Ga_2O_3 = 2Ga(l) + 3MgO + 3Cl_2(g)$ | 1.298 |
| $MgCl_2 + ZnO = Zn(l) + MgO + Cl_2(g)$ | 1.259 |
| $3MgCl_2 + WO_3 = W + 3MgO + 3Cl_2(g)$ | 0.984 |
| $2MgCl_2 + GeO_2 = Ge + 2MgO + 2Cl_2(g)$ | 0.977 |
| $2MgCl_2 + SnO_2 = Sn(l) + 2MgO + 2Cl_2(g)$ | 0.944 |
| $3MgCl_2 + Fe_2O_3 = 2Fe + 3MgO + 3Cl_2(g)$ | 0.939 |
| $2MgCl_2 + MnO_2 = Mn + 2MgO + 2Cl_2(g)$ | 0.855 |
| $3MgCl_2 + MoO_3 = Mo + 3MgO + 3Cl_2(g)$ | 0.824 |
| $3MgCl_2 + Sb_2O_3 = 2Sb(l) + 3MgO + 3Cl_2(g)$ | 0.749 |
| $MgCl_2 + NiO = Ni + MgO + Cl_2(g)$ | 0.743 |
| $4MgCl_2 + Co_3O_4 = 3Co + 4MgO + 4Cl_2(g)$ | 0.655 |
| $3MgCl_2 + Bi_2O_3 = 2Bi(l) + 3MgO + 3Cl_2(g)$ | 0.488 |
| $MgCl_2 + CuO = Cu + MgO + Cl_2(g)$ | 0.316 |



a mix of molten salts can also further decrease the solubility of MgO.[14,15] The solubility of MgO in pure $MgCl_2$ at 730 °C was reported to be about 0.36 mol%, which is fairly low in contrast with $CaCl_2$ (>20 mol% at 850 °C) and LiCl (>10 mol % at 650 °C).[16,17] However, if 70 mol% NaCl was added, the solubility of MgO can be significantly decreased to about 0.01 mol%. On the other hand, the solubility of MgO in equimolar NaCl–KCl at 730 °C is also less than 0.01 mol%.[18] These data suggest that using the molten mixture of $MgCl_2$–NaCl–KCl (MNK) can be more effective for disengaging the carbon anode from $O^{2-}$ ions.

In this work, we further demonstrate our new process by the electrolysis of $Ta_2O_5$ in the MNK melt at 700 °C. The mechanism of $Ta_2O_5$ reduction was investigated, and nanometer Ta powder (<50 nm) was produced at an energy consumption of about 1.0 kW h $kg_{Ta}^{-1}$. The inert graphite anode was confirmed with the anodic gaseous products analysed in detail.

## Experimental

Anhydrous $MgCl_2$, NaCl, and KCl (analytical grade, Tianjin Guangfu Fine Chemical Research Institute, or Sinopharm Chemical Reagent Co., Ltd, China) were mixed in the eutectic ratio 5 : 3 : 2 (in mole ratio and 5 mol in total amount), and heated in a graphite or alumina crucible (inner diameter: 25–50 mm; height:

200–700 mm) in a programmable vertical furnace equipped with a sealable stainless steel retort (Wuhan Experimental Furnace Plant). The furnace temperature was slowly raised to and maintained at 400 °C for more than 12 h, and then to 700 °C until the salt mixture was fully molten. Pre-electrolysis of the molten salt was applied at 1.6 V to remove moisture and other redox-active impurities with the graphite crucible (or a graphite rod of 10 mm diameter in the alumina crucible) as the anode and a Mo wire (diameter: 2 mm) as the cathode. Pre-electrolysis lasted (*ca.* 10 h) until the current reached a low and stable background level.

Cyclic voltammograms (CVs) were recorded using a Mo cavity electrode (MCE) loading with $Ta_2O_5$ powder, with the potential reference to a quartz sealed Ag/AgCl electrode. For constant potential, constant cell voltage and galvanostatic electrolysis, $Ta_2O_5$ powder (analytical grade; particle sizes: 300 nm; Zhuzhou Cemented Carbide Works Imp. & Exp. Company) was individually die-pressed into cylindrical pellets (10 MPa, 13 or 20 mm in diameter, 0.7–2 g: 1.1–1.7 mm in thickness, porosity: ~50%), sintered in air at 1000 °C for 2 h, and sandwiched between two molybdenum (Mo) meshes to form an assembled cathode. After electrolysis for a designated time, the cathode was removed from the furnace, cooled in argon, washed in distilled water, or in dilute HCl (0.1 mol $L^{-1}$) and water again, and then dried in a vacuum at 80 °C before further analyses. The CVs were recorded using CHI660A Electrochemical System (Shanghai Chenhua, China), while the electrolysis was controlled by a multichannel four-electrode potentiostat (Neware, China).

The products were characterised by X-ray diffraction spectroscopy (X-ray 6000 with Cu K$\alpha$1 radiation at $\lambda = 1.5405$ Å, Shimadzu, Japan), and a FEI Sirion Field Emission Gun SEM system. GC (FULI 9790II, with a thermal conductivity detector and argon serving as a carrier gas) was used for the analysis of the anodic gaseous products. Ion Chromatography (IC) analysis for $Cl^-$ ions was carried out using METROHM 881 Compact IC pro, with the $ClO^-$ ions reduced to $Cl^-$ ions by $H_2O_2$.

## Results and discussion

Fig. 1 shows the cyclic voltammogram (CV) of $Ta_2O_5$ powders in MNK at 700 °C using the metallic cavity electrode (MCE). For comparison, a CV recorded on an empty MCE is superimposed. No significant reaction current can be observed on the blank CV before Mg deposition (C0) and dissolution, with an $Mg/Mg^{2+}$ equilibrium potential of about −1.55 V *vs.* Ag/AgCl. The reduction current of $Ta_2O_5$ was found initially to be −0.4 V *vs.* Ag/AgCl. Preliminary comparison and analysis of the CVs of $Ta_2O_5$ in molten MNK and those previously reported in $CaCl_2$ have revealed fairly similar main reduction features, showing mainly three reduction processes (C1–C3).[19] However, the starting potential of C3 is unclear due to the overlap with C2.

According to Table 1, the reduction of $Ta_2O_5$ to Ta could occur at a potential about 0.9 V more positive than the deposition of Mg, thus, potentiostatic electrolysis of $Ta_2O_5$ was performed at −0.8 V *vs.* Ag/AgCl, a potential 0.75 V more positive than the Mg deposition potential so Ta was predicted to be produced. The current–time plot is shown in Fig. 2a. The reduction current rises initially to a peak suggesting the reduction followed the propagation of the three-phase interlines, which was generally observed during reduction of insulating oxides to metals.[20]

 

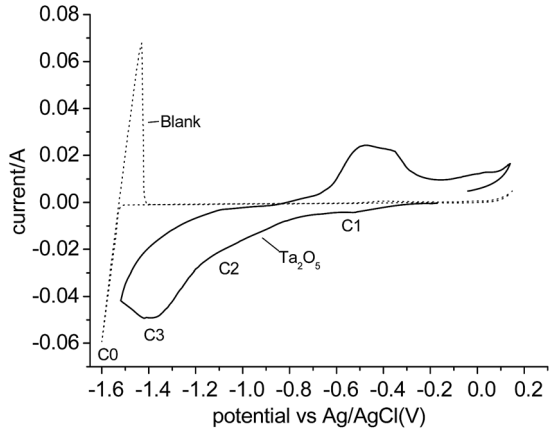


Fig. 1 Cyclic voltammograms (CVs) of the blank MCE and the MCE loading with $Ta_2O_5$ powder in molten $MgCl_2$–NaCl–KCl at 700 °C.

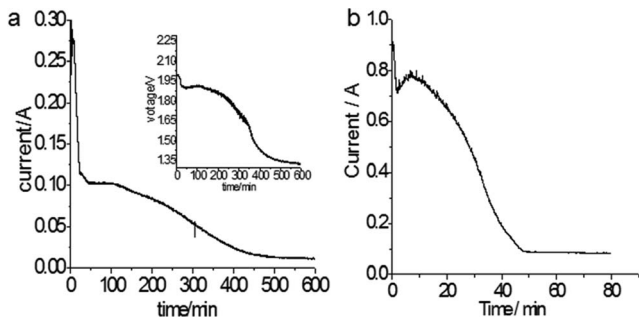


Fig. 2 Current–time plots of (a) potentiostatic electrolysis of a $Ta_2O_5$ pellet in MNK at −0.8 V *vs.* Ag/AgCl and 700 °C. Insert: corresponding cell voltage profile. (b) Constant voltage electrolysis of a 0.7 g $Ta_2O_5$ pellet at 2.0 V and 700 °C.

In line with the CV, Fig. 2a also shows several reduction processes. The first reduction displayed a high reduction current of about 0.25 A in the initial 30 minutes. The second reduction corresponded to the plateau current at about 0.1 A, which began to decrease at about 110 minutes, then a slope change at about 250 minutes could indicate a third reduction process. Finally, the current levelled off to background current after 500 minutes. To identify these reductions, XRD patterns of the electrolysis products after different times were scanned and displayed in Fig. 3. It can be seen that after 27 minutes, the $Ta_2O_5$ was almost completely reduced to $TaO_2$. The electrolysis product at 300 minutes included Ta and $Mg_4Ta_2O_9$. The appearance of $Mg_4Ta_2O_9$ after $TaO_2$ may suggest the possible disproportionation reaction of $TaO_2$, possibly like its congener $VO_2$, and the generation of an excess of MgO may have shifted the reaction to form the stabilized $Mg_4Ta_2O_9$. The final electrolysis product after washing with water consisted of Ta and MgO. The presence of MgO in the cathode indicates its low solubility in the MNK melts as discussed above.

The cell voltage (the inset in Fig. 2a) during the −0.8 V constant potential electrolysis was also monitored. In the main reduction stage of $Ta_2O_5$, the cell

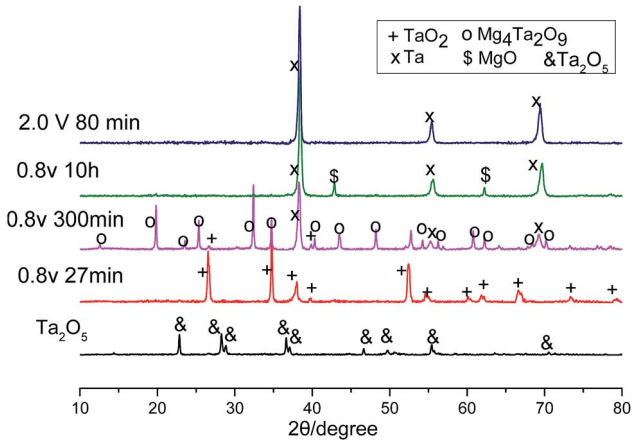


Fig. 3 XRD patterns of the products collected at the indicated times of potentiostatic electrolysis (−0.8 V *vs.* Ag/AgCl, water washed only) and constant voltage electrolysis of $Ta_2O_5$ (2.0 V, water and acid washed) at 700 °C in MNK.

voltage was about 1.9 V, which was reasonably higher than the decomposition voltage ~1.64 V of $Ta_2O_5$ in the $MgCl_2$ based melt as calculated in Table 1. In addition, it can be seen that after the cell voltage decreased to about 1.64 V, it dropped suddenly. These may indicate that the electrolysis was mainly *via* the assumed Reaction (4) or specifically Reaction (7) for $Ta_2O_5$:

$$5MgCl_2 + Ta_2O_5 = 2Ta + 5MgO + 5Cl_2(g) \quad (7)$$

Constant cell voltage electrolysis at 2.0 V was also carried out, and the current–time plot is shown in Fig. 2b. It can be seen that the reduction completed in about 50 minutes, and the dimensions of the cathode pellet remained almost unchanged before and after the reduction (Fig. 4a), suggesting the possibilities of both high electrolysis speed and high Ta recovery (nearly 100% in this work). Mass analysis was carefully carried out after the product was washed with water and 0.1 mol $L^{-1}$ HCl respectively, and this confirmed that most of the MgO

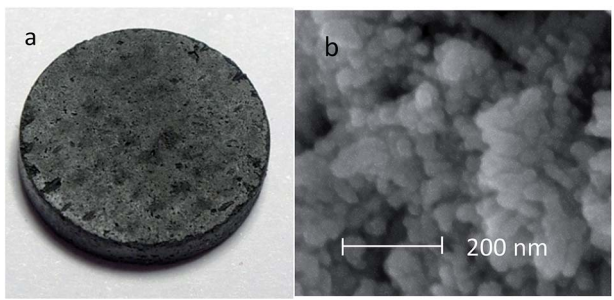


Fig. 4 (a) $Ta_2O_5$ pellet collected after 80 min electrolysis in 700 °C MNK at 2.0 V. (b) Scanning Electron Microscopy (SEM) image of the Ta nanoparticles shown in (a) (after acid washing).

 

generated through Reaction (7) stayed in the cathode. It is interesting that although the porosity of the $Ta_2O_5$ pellet was only about 50% of that which is commonly used for electro-reduction in molten $CaCl_2$, the influence of MgO accumulation in the oxide cathode was insignificant for the electro-reduction. However, it can be derived that the porosity of the $Ta_2O_5$ cathode needs to be higher than 30% to prevent the ion passages from becoming blocked.

On the other hand, although the cathode pellet taken out from the molten salt was perfectly strong, it dispersed to a powder after washing in water. After being further washed with acid, pure Ta was obtained, and the XRD pattern is shown in Fig. 3. The SEM images show very fine particles (~50 nm) of the resulting Ta powder, which were smaller than those produced in molten $CaCl_2$ at 900 °C, suggesting higher specific capacitance.[19] This phenomenon may be partly associated with the relatively low molten salt temperature (700 °C) and also partly attributed to the MgO precipitated inside the pellet which prevented physical sintering of the Ta particles. The current efficiency was higher than 92%, with an energy consumption of about 1.3 kW h $kg_{Ta}^{-1}$ for the electrolysis of 0.7 g $Ta_2O_5$ and 1 kW h $kg_{Ta}^{-1}$ for the electrolysis of 2 g $Ta_2O_5$.

On the graphite anode, for verification of chlorine evolution, galvanostatic electrolysis of $Ta_2O_5$ at 1.5 A was performed in MNK. Since the MNK melt does contain some $O^{2-}$ ions, although with a concentration in the order of $10^{-4}$ in molar fraction, the discharge of $O^{2-}$ ions on graphite would occur. According to Scheme 1, the amounts of $O_2$, $CO_2$, CO and $Cl_2$ in the anodic gaseous product were determined.

First, about 500 mL of anodic gas was collected as shown in Fig. 5a. The colour of the anodic product was yellowish green. This is straightforward evidence for formation of $Cl_2$ on the anode. After being absorbed by NaOH solution, a starch iodide test indicated the existence of $ClO^-$ in the solution, again convincing evidence for anodic $Cl_2$ gas, which has been reacted with NaOH. In addition, ion chromatography (IC) analysis indicated that the $Cl^-$ and $ClO^-$ ion concentration in the NaOH solution approximately matched the absorbed gas volume (about 460 mL). About 40 mL colourless gas remained, and GC analysis (Fig. 6) indicated the existence of $O_2$ and CO with concentrations in the total anodic gas of about 1.2 mol% and 0.2 mol%, respectively.

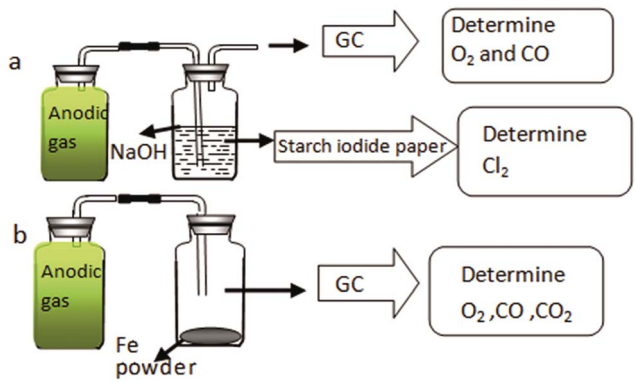


Scheme 1 Illustration of the method for identification of anodic gas.

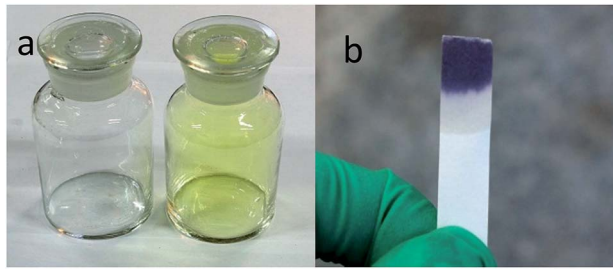


Fig. 5 (a) Bottles with 500 mL air (left) and anodic gas (right). (b) Photo of the colour change of the starch iodide paper after immersing into anodic gas bubbled through NaOH solution.

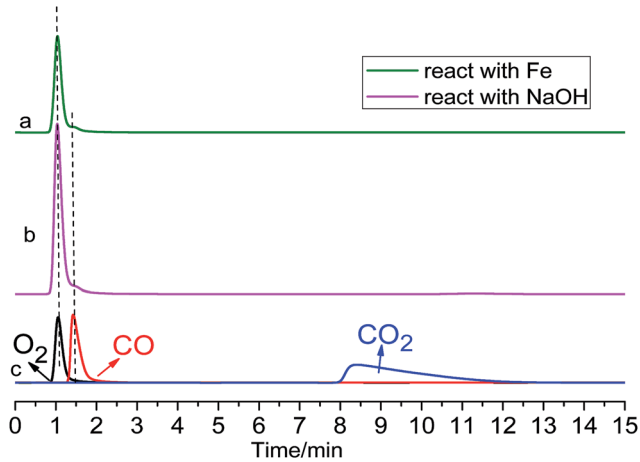


Fig. 6 GC spectrogram of anodic gas. Line (a): after reacting with Fe powder. Line (b): after being absorbed by NaOH solution. Line (c): superimposed GC spectrograms of pure $O_2$, CO and $CO_2$.

No $CO_2$ was detected by GC, however, even if it was formed on a graphite anode, according to the $Cl_2$ volume indicated by IC, the $CO_2$ concentration would be very low. Similarly, it was reported that no $CO_2$ gas was found as an anodic product during electrolysis of MgO in $MgCl_2$–$NdCl_3$ system at 700 °C.[21] However, it seems strange that there was $O_2$ as an anodic product without $CO_2$ gas on a graphite anode. For confirmation, we designed another experiment. As shown in Scheme 1b, the anodic gaseous product was allowed to react with the reducing Fe powders thoroughly, and the remaining colourless gas was also detected by GC. According to Fig. 6, $CO_2$ was in truth absent in the anodic product.

According to the above tests, the composition of the anodic gaseous product during galvanostatic electrolysis of $Ta_2O_5$ at 1.5 A consisted of mainly $Cl_2$ gas, about 1 mol% $O_2$ gas and trace amounts of CO gas, as summarized in Table 2. No $CO_2$ was formed on the graphite anode.

To determine the origination of anodic $O_2$ gas, CVs of the graphite electrode in the MNK melt were recorded as shown in Fig. 7. According to Fig. 7, the evolution

 

Table 2 Composition of the anodic gaseous product during galvanostatic electrolysis of $Ta_2O_5$ at 1.5 A

| Compositions | Content (mol%) |
|---|---|
| $Cl_2$ | 98.6 |
| $O_2$ | 1.2 |
| CO | <0.2 |
| $CO_2$ | None |

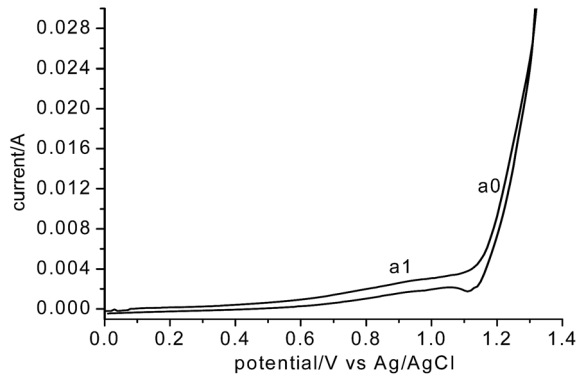


Fig. 7 Cyclic voltammogram of graphite in eutectic $MgCl_2$–NaCl–KCl (700 °C) *vs.* Ag/AgCl, scan rate 200 mV $s^{-1}$.

of chlorine (a0) was initiated at 1.1 V *vs.* Ag/AgCl. Coupled with the deposition potential of Mg (see Fig. 1a) on MCE, the decomposition voltage of $MgCl_2$ was determined to be 2.65 V, which is fairly close to the thermodynamic value (2.534 V) calculated from HSC Chemistry 6. The measured value was slightly higher, which is reasonable considering that the molar fraction of $MgCl_2$ in the MNK was only 0.5. The current corresponding to chlorine evolution increased rapidly with the positive scan, indicating that there is no kinetic difficulty on the discharge of $Cl^-$ ions on a graphite anode. Since $Cl^-$ ions are the main anions in the MNK melt, concentration polarization for the chlorine evolution is also negligible. On the contrary, in molten $CaCl_2$, the anodic discharge of $O^{2-}$ ions on graphite is well known to be kinetically difficult both in terms of charge transfer and mass transfer.

Before a0, there is an apparent anodic current at a1, which is very stable according to the multi-cycle scans and could be attributed to the discharge of $O^{2-}$ ions on the graphite anode. However, unlike the discharge of $O^{2-}$ on a carbon based anode in molten $CaCl_2$, which exhibited complicated voltammograms involving formation of $CO_2$, CO and $O_2$ gases,[22–24] here the CVs of $O^{2-}$ discharge in MNK featured a single reaction, probably the formation of $O_2$ gas as mentioned above. To confirm it, potentiostatic electrolysis was performed at 1.0 V *vs.* Ag/AgCl against a $Ta_2O_5$ pellet cathode. The anodic current remained very stable at about 15 mA during the total 3 hour electrolysis. However, no anodic gas has automatically flowed out from the anodic gas chamber. The chamber was then sealed and the anodic gas was sampled at different times for GC analysis.

Fig. 8 shows the GC analysis results. As can be seen, after 0.5 h electrolysis, there was a small peak of $O_2$ gas but no CO and $CO_2$ gas was found. After about 1 h electrolysis, the $O_2$ concentration increased significantly, and small peaks of CO and $CO_2$ became just perceptible, and the $O_2$ : CO : $CO_2$ ratio was about 8.2 : 1.3 : 0.5, which changed to 7.9 : 1.0 : 1.1. Considering initially there is only $O_2$ evolution and the $CO_2$ content became larger and larger, it is likely that the formation of $CO_2$ is a result of a reaction between the graphite anode and the accumulated $O_2$ in the anodic chamber. Combining the CV result and the GC analysis of the anodic gas during constant potential electrolysis at 1.0 V, it might be reasonable that the a1 current in Fig. 7 corresponds to the discharge of $O^{2-}$ ions to $O_2$ gas on the graphite anode in the MNK melt at 700 °C. However, the small steady current (15 mA) at 1.0 V *vs.* Ag/AgCl was most likely to be the limited diffusion current of $O^{2-}$ ion discharge, which is only about 1.5% of the total current considering a 1.0 A $g^{-1}$-$Ta_2O_5$ or higher current would be applied in the actual electrolysis.

The optical images of the graphite anode before and after repeated electrolysis for *ca.* 100 h in the eutectic MNK melt were compared in Fig. 9. In line with the $Cl_2$ and $O_2$ gas evolution at the anode, the fine spiral machining marks of *ca.* 100 nm in width on the side of the graphite rod remained almost intact, even though these protruding parts are usually the most vulnerable sites to chemical or electrochemical attack. These observations suggested that the graphite anode is basically inert during the electrolysis of solid oxide cathode in the $MgCl_2$ based molten salts. However, it is well-known that the anodic reaction of the solid oxide cathode electrolysis at a graphite electrode in $CaCl_2$ was the discharge of the $O^{2-}$ to carbon oxides and carbonate ions, leading to significant erosion of the graphite anode, shuttle reactions of the oxygenated species ($O^{2-}$ and $CO_3^{2-}$), and formation of a thick layer of floating carbon powder on the surface of the molten electrolyte. Since there was no corrosion to the graphite anode and consequently no carbon generated on the cathode due to the reduction of $CO_3^{2-}$ in a $MgCl_2$ based electrolyte, no floating carbon was supposed to form on the surface of molten MNK. This was confirmed by the clear surface of MNK after 100 h electrolysis of $Ta_2O_5$ as shown in Fig. 9c.

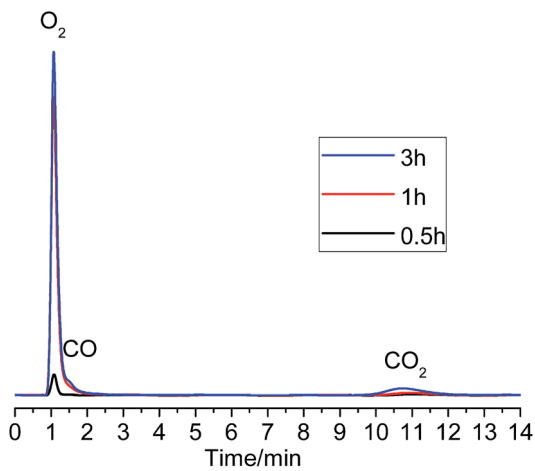


Fig. 8 GC spectrograms of anodic gas produced by potentiostatic polarization of graphite in 700 °C MNK at 1.0 V *vs.* Ag/AgCl (time indicated).

 


Fig. 9 Optical photos of the graphite rod anode (dia. 2.0 cm) (a) before and (b) after electrolysis experiments for *ca.* 100 h in the eutectic MNK melt. (c) Photo of cooled MNK salts after 100 h electrolysis of $Ta_2O_5$.

These results indicate that both the graphite anode and the MNK salt are ready for lengthy electrolysis. Of course, the consuming $MgCl_2$ needs to be supplemented, for example, along with the metal oxide pellet. In addition, the $Cl_2$ gas has many applications and can be collected as already commercially demonstrated in the chlor-alkali industry and the electrolysis of molten LiCl and $MgCl_2$. It is also possible to use the $Cl_2$ gas to regenerate $MgCl_2$, noting the recent progress in developing $H_2$–$Cl_2$ fuel cells,[25] which generate electricity and HCl while HCl is needed to convert MgO in the cathode back to $MgCl_2$.

## Conclusions

We have demonstrated the high speed, low energy consumption electrolysis of $Ta_2O_5$ in $MgCl_2$–NaCl–KCl melt using an inert graphite anode. The reduction process was investigated by cyclic voltammetry, and potentiostatic and constant voltage electrolysis. The main intermediate products of the electro-reduction of $Ta_2O_5$ were identified to be $TaO_2$ and $Mg_4Ta_2O_9$. The final reduction product was nanometer Ta powder with sizes of about 50 nm. The anodic product included mainly $Cl_2$ gas, plus about 1 mol% $O_2$. There was only about 0.2 mol% CO in the anodic gas, and no $CO_2$ was detected, suggesting that the graphite anode is fairly stable in our new process. The process should be applicable for the preparation of many other metals and alloys with high energy efficiency and low carbon emission.

## Acknowledgements

We thank the NSFC, Ministry of Education of China, the EPSRC, Guangdong Nat. Sci. Found., Nat. Key Fundamental R&D Program of China and Nat. Hi-Tech R&D Program of China for financial support (Grant No. 20773094, 21173161, 51204060, NCET-11-0397, EP/J000582/1, S2012040007501).

# References

1 W. Kroll, *Trans. Electrochem. Soc.*, 1940, **78**, 35–47.
2 T. Okabe, K. Nikami and K. Ono, *Bulletin of the Iron and Steel Institute of Japan*, 2002, **7**, 39–45.
3 G. Z. Chen, D. J. Fray and T. W. Farthing, *Nature*, 2000, **407**, 361–364.
4 D. H. Wang, X. B. Jin and G. Z. Chen, *Annu. Rep. Prog. Chem., Sect. C: Phys. Chem.*, 2008, **104**, 189–234.
5 A. M. Abdelkader, K. T. Kilby, A. Cox and D. J. Fray, *Chem. Rev.*, 2013, **113**, 2863–2886.
6 L. Cassayre, P. Palau, P. Chamelot and L. Massot, *J. Chem. Eng. Data*, 2010, **55**, 4549–4560.
7 C. Schwandt and D. Fray, *Electrochim. Acta*, 2005, **51**, 66–76.
8 D. R. Sadoway, *JOM*, 2001, **53**, 34–35.
9 K. T. Kilby, S. Jiao and D. J. Fray, *Electrochim. Acta*, 2010, **55**, 7126–7133.
10 C. Chen and X. Lu, *Acta Metall. Sin. (Chin. Ed.)*, 2008, **44**, 145.
11 S.-W. Kim, E.-Y. Choi, W. Park, H. S. Im and J.-M. Hur, *Electrochem. Commun.*, 2015, **55**, 14–17.
12 S. Jiao, K.-N. P. Kumar, K. T. Kilby and D. J. Fray, *Mater. Res. Bull.*, 2009, **44**, 1738–1742.
13 W. Li, Y. T. Yuan, H. L. Chen, X. B. Jin, Z. Y. Wang and G. Z. Chen, *Progress in Natural Science: Materials International*, 2015, **11**, 002.
14 S. Boghosian, A. Godø, H. Mediaas, W. Ravlo and T. Østvold, *Acta Chem. Scand.*, 1991, **45**, 145.
15 K. H. Sten, *Electrochim. Acta*, 1979, **24**, 509.
16 T. Usami, M. Kurata, T. Inoue, H. E. Sims, S. A. Beetham and J. A. Jenkins, *J. Nucl. Mater.*, 2002, **300**, 15.
17 D. A. Wenz, I. Johnson and R. D. Wolson, *J. Chem. Eng. Data*, 1969, **14**, 250.
18 R. Combes, F. De Andrade, A. De Barros and H. Ferreira, *Electrochim. Acta*, 1980, **25**, 371–374.
19 T. Wu, X. B. Jin, W. Xiao, X. H. Hu, D. H. Wang and G. Z. Chen, *Chem. Mat.*, 2007, **19**, 153–160.
20 G. Z. Chen, E. Gordo and D. J. Fray, *Metall. Mater. Trans. B*, 2004, **35**, 223.
21 K. Cathro, R. Deutscher and R. Sharma, *J. Appl. Electrochem.*, 1997, **27**, 404–413.
22 H. L. Chen, X. B. Jin, L. P. Yu and G. Z. Chen, *J. Solid State Electrochem.*, 2014, **18**, 3317.
23 M. Mohamedi, B. Børresen, G. M. Haarberg and R. Tunold, *J. Electrochem. Soc.*, 1999, **146**, 1472–1477.
24 R. Tunold, G. M. Haarberg, K. S. Osen, A. M. Martinez and E. Sandnes, *ECS Trans.*, 2011, **35**, 1–9.
25 B. Huskinson, J. Rugolo, S. K. Mondal and M. J. Aziz, *Energy Environ. Sci.*, 2012, **5**, 8690.

 